Influence of cooling rate on deformation due to effective stress in a solidifying alloy

QIUPING YU
AuPeace Technology Services, Inc., P. O. Box 3599, Worcester, MA 01613, USA
E-mail: qiuping-y@hotmail.com

DIRAN APELIAN
Metal Processing Institute, Worcester Polytechnic Institute, Worcester, MA 01609, USA

The relative volume rate at a local volume element, div $\boldsymbol{V}_S'$, that is used to evaluate the deformation in the two-phase zone of a solidifying alloy, is dependent on history of the effective stress. In a model of unidirectional solidification, the variation of the effective stress with x-direction or time at the fast cooling rate is larger than the one at the slow cooling rate. The different relative volume rates due to the inhomogeneous cooling rates produce deformation mismatch among the various volume elements in an ingot. It is suggested that accumulation of the deformation mismatch gives rise to thermal residual stain and stress, and hot-tearing tendency in the ingot. The effective stress may be residual in the solidified alloy if it is less than the strength of the alloy itself at the fast cooling rate, and may be relaxed by the deformation of the two-phase zone and play a role in forming the channel space filled with the unstable flow at the slow cooling rate. © *2000 Kluwer Academic Publishers*

Nomenclature

a_E	constant in Equation 15b
A	viscosity constant
b_{Ex}	constant in Equation 15b
b_{Lx}	constant in Equation 15a
C_a	local average concentration (wt %)
C_S	local solid concentration (wt %)
C_L	liquid concentration (wt %)
E	elastic modulus (GPa)
g_L	volume fraction liquid
g_S	volume fraction solid
ΔG_{VIS}	Activation energy of viscosity
k	equilibrium partition ratio
m	solid-solid contact coefficient
m_L	liquidus slope (K/wt %)
p	pressure (kPa)
p_0	ambient pressure (kPa)
q	constant in Equation 15
R	gas constant
t	time (s)
T	temperature (K)
T_E	solidus temperature (K)
T_L	liquidus temperature (K)
U_b	volume of an element in two-phase zone (m^3)
$\boldsymbol{V}_L$	liquid velocity in two-phase zone (m s^{-1})
$\boldsymbol{V}_S$	solid velocity in two-phase zone (m s^{-1})
$\boldsymbol{V}_S'$	solid velocity weighing by g_S (m s^{-1})
x_E	position of the eutectic isotherm
x_L	position of the liquidus isotherm

Greek Symbols

α	compressibility coefficient (N^{-1} m^2)
β	solidification shrinkage
γ	strain
ε	cooling rate (K s^{-1})
η	viscosity (Pa s)
ρ_a	average density (kg m^3)
ρ_L	liquid density (kg m^3)
ρ_S	solid density (kg m^3)
σ	total stress (kPa)
σ'	effective stress (kPa)
σ_E'	effective stress due to elastic behavior (kPa)
σ_S	solid stress (kPa)
σ_V'	effective stress due to viscous behavior (kPa)

1. Introduction

Solidification shrinkage and contraction(or expansion) always exist in a solidifying alloy, and may result in such solidification defects as thermal residual strain and stress, segregation, and hot tear, which also related to the alloy composition and the solidification conditions. Normal solidification processing is carried out at elevated temperature and thermal residual stress *etc*. are generated as the alloy is cooled from the processing temperature. These defects occur in as-cast ingots as well as in advanced materials such as composites [1, 2]. Prediction of thermal residual strain and stress, segregation, and hot tear is of great importance for evaluating and designing the various properties of

materials. Deformation of the two-phase zone during solidification results in these defects, and it is necessary to develop models for understanding the deformation mechanism.

In his analysis of hydrostatic tensions in solidifying materials, Campbell [3, 4] proposed that various models for the evaluation of the negative pressures which may occur in the solidifying materials which exhibit various deformation modes: elastic-plastic, Bingham, viscous, or creep flow. For metal alloys, the solution of the creep flow model seems to be more reliable than that of the elastic-plastic one. The solidification rate was considered since this critically affects both the flow of the liquid and the creep of the solid, and the very high stresses predicted by the spherically symmetric creep model are a direct consequence of the very high solidification rate as freezing nears completion in a sphere. The experimental and theoretical studies of solid movement and deformation in the two-phase zone were carried out by Flemings and Rosenberg *et al*. [5–7]. The fraction solid at which the dendrites form a cohesive network, and at which the network begins to develop some strength, depends on dendrite size and morphology, but a number of studies in different alloys show it to be in the range of about 0.1 to 0.2 and occasionally higher. Above 0.2 fraction solid, shear strength increases with increasing fraction solid, and is found also to increase somewhat with increasing strain rate and with increasing grain size. In well grain-refined alloys, strength does not begin to develop until 0.4 fraction solid. The developing strength of the solid network can cause localized strains with resultant formation of highly segregated regions, or open hot tears. When metal can no longer mass feed to the hot spot in a casting, the contraction strains pull the solid dendrites apart at this location. If the casting is well fed, there is now a stage when liquid flow between the separating dendrites to heal the incipient tears, and regions of segregation result. As solidification proceeds, a time is reached when liquid can no longer flow to compensate for the strain. At this stage, if the strain continues, open fractures result which are termed hot tears. Alternately, the casting might develop enough strength at this point to resist tearing. Resistance to hot-tearing is related to the alloy composition. Minimum resistance to hot-tearing is found in many alloys at compositions intermediate between the pure metal and a eutectic composition. Another factor affecting hot-tearing resistance is grain size: the finer the grain size, the greater the resistance.

The cooling rate is a parameter that is often used to describe the as-cast microstructure, especially the primary and the secondary dendrite arm spacing, and the solidification rate and temperature gradient across the solidifying interface are the parameters which actually describe the morphology of the interface growth, the local solute diffusion, and kinetic processes [7–9]. The influence of cooling rate on interdendritic fluid flow in the two-phase zone was investigated: when isotherms move fast at a large cooling rate such as greater than $10^{-1\circ}\mathrm{Cs}^{-1}$, the siphonic force due to solidification shrinkage mainly results in the interdendritic flow and gravity acting on a fluid of variable density cannot play an effective role so that natural convection in the mushy zone is not evident; with decreasing the cooling rate, movement of the isotherms is gradually getting slow, and the gravity force can change the flow direction and cause the back-flow due to natural [10]. Modeling of thermal residual strain and stress and hot-tearing tendency in a solidifying alloy has been carried out in recent years. Criteria based on the difference in cooling rate between the surface and the center of a solidifying ingot and based on the level of tensile stress (normalized by dividing the computed stress by the yield stress for the local temperature) were used to predict conditions and locations likely to hot tear to form radial cracks [11, 12]. Kim *et al*. [13] proposed that solidification contraction, which is related to a linear coefficient of thermal expansion, for deformation analysis of an aluminum alloy is proportional to the local solidification time; when the same solidification contraction was input for all meshes in analysis, the casting did not show inward deformation, while different solidification contraction with location in the casting was input the casting did. It should be pointed out that the definition of solidification contraction is not very clear, e. g, the relationship between solidification contraction and solidification shrinkage.

The purpose of this paper is to investigate the effect of cooling rate during solidification on the thermal residual strain and stress and the hot-tearing tendency on the basis of the effective stress analysis. The concept of the effective stress stems from a new approach to the local solute redistribution equation [14]. In the following sections, the theoretical models will be described first, that includes: (1) the modified local solute redistribution equation, (2) relationship of the new term $\mathrm{dis}V_S'$ in the equation with the effective stress, and (3) the model for calculating the effective stress. For given solidification model, the effect of cooling rate on deformation of the two-phase zone will be discussed on the basis of the calculated results under the two cooling conditions.

2. Theoretical models

2.1. The modified local solute redistribution equation

The basic equation for describing the effect of solid movement on solute redistribution is developed on the basis of models of continuum approach to a porous media. Assumptions for the original local solute redistribution equation are as follows [15, 16]. (1) A small volume element in the two-phase zone is large enough that the fraction solid within it any time is exactly the local average, but small enough that it can be treated as a differential element. (2) There is no movement of the solid phase into or out off the element. (3) Solute enters or leaves the element only by liquid flow to feed shrinkage. (4) Mass flow in or out of the element by diffusion is merged into the fluid flow. (5) Solidification occurs with equilibrium at the solid-liquid interface so that there is no undercooling, and the rate of solidification is controlled only by the rate of heat transfer and convection within the two-phase zone. (6) the local temperature and the composition of the solid at the interface are specified by the local composition of the

liquid. (7) Diffusion in the solid is negligible. (8) Solid density is constant. (9) No pore forms during solidification.

The research in this paper is based on relaxing the assumption (2) and (3), that is, movement of the solid phase in the two-phase zone , and solute into or out of the element by solid movement as well as by liquid flow will be considered. For solidification occurring in each volume element treated as porous medium, where liquid flow and solid movement occur through and in it, the mass conservation equation and the solute conservation equation should be given as, respectively:

$$\frac{\partial \rho_a}{\partial t} = -\nabla \cdot (\rho_a \boldsymbol{V}) \tag{1}$$

and

$$\frac{\partial (\rho_a C)}{\partial t} = -\nabla \cdot (\rho_a C_a \boldsymbol{V}) \tag{2}$$

where ρ_a is average density ($=g_L\rho_L + g_S\rho_S$), g_L and g_S are volume fraction liquid and volume fraction solid, respectively, ρ_L and ρ_S are liquid and solid densities, respectively, t is time, $\boldsymbol{V}$ is velocity of the two-phase zone, C is concentration, and C_a is local average concentration ($=g_L C_L + g_S C_S$), C_L and C_S are liquid and solid concentration, respectively. Combining Equations 1 and 2 provides a new expression for solute redistribution under the conditions of all other assumptions for the original local solute redistribution equation except for changing the assumptions (2) and (3) [14]:

$$\frac{1}{g_L}\left[\frac{\partial g_L}{\partial t} - \mathrm{div}(g_S \boldsymbol{V}_S)\right] = -\frac{1-\beta}{1-k}\left(1 + \frac{\boldsymbol{V}_L - \nabla T}{\varepsilon}\right)\frac{1}{C_L}\frac{\partial C_L}{\partial t} \tag{3}$$

where $\boldsymbol{V}_L$ and $\boldsymbol{V}_S$ are liquid and solid velocities in the two-phase zone, respectively, β is solidification shrinkage ($= -(\rho_L - \rho_S)/\rho_S$), k is equilibrium partition ratio, ε is cooling rate, and C_L is liquid concentration.

Equation 3 is a new equation considering solid movement in the two-phase zone, in which the term $1/g_L[\partial g_L/\partial t\text{-div}(g_S \boldsymbol{V}_S)]$ replaces the one $1/g_L(\partial g_L/\partial t)$ in the original local solute redistribution equation. In the left side of Equation 3, $\partial g_L/\partial t$ is the local derivative that expresses the rate of change of g_L with time at a fixed point of the two-phase zone, and $\mathrm{div}(g_S \boldsymbol{V}_S)$ is a new term. $\boldsymbol{V}_S$ is velocity of solid movement (or deformation) at the point of the two-phase zone, and $g_S \boldsymbol{V}_S$ can be regarded as the solid velocity weighted by volume fraction solid at the point. For convenience, there is:

$$\boldsymbol{V}_S' = g_S \boldsymbol{V}_S \tag{4}$$

For a two-phase zone treated as porous medium, a volume of element of the two-phase zone is U_b and velocity of the solid network in the element is $\boldsymbol{V}_S'$. According to the concept of total derivative, there is:

$$\mathrm{div}\, \boldsymbol{V}_S' = \frac{1}{U_b}\frac{\mathrm{d}U_b}{\mathrm{d}t} \tag{5}$$

that is, the term $\mathrm{div}\, \boldsymbol{V}_S'$ is defined as relative volume rate at a local volume element. The method proposed by Bear [17] is used to deal with the relation of $\boldsymbol{V}_S'$ to the effective stress. The term $\mathrm{div}\, \boldsymbol{V}_S'$ is dependent on history of the effective stress acting on the solid phase of the two-phase zone:

$$\mathrm{div}\, \boldsymbol{V}_S' = -\alpha \frac{\mathrm{d}\sigma'}{\mathrm{d}t} \tag{6}$$

where α is compressibility coefficient, and σ' is the effective stress.

2.2. The effective stress

The total load of the liquid-solid phase zone is balanced by interparticle stress in the solid phase and by pressure in the liquid phase according to Terzaghi's theory [17, 18]. For contact areas of the solid and liquid phases with each other, there is:

$$\sigma = (1-m)p + m\sigma_S \tag{7}$$

where σ is total stress, p is pressure, and σ_S is solid stress, and m is solid-solid contact coefficient. The effective stress acting on the solid phase σ' is defined as:

$$\sigma' = m\sigma_S \tag{8}$$

In the above equations, a positive pressure ($p > 0$) means compression. Similarly, σ and σ' are taken as positive in the equations when they are compressive stresses.

The effective stress σ' is dependent on the solid-solid contact coefficient m, that is dependent on the volume fraction solid for a certain casting structure such as equiaxed grain. When g_S is small such as less than 0.2, the solidification of an alloy lies in the stage of mass feeding, in which there is little contact among the solid-phase grains in the two-phase zone, and m seems to be zero. With increasing the volume fraction solid, the contact among them increases and the value of m is enhanced. When g_S is equal and more than 0.2, the value of m is:

$$m \equiv g_S^n \tag{9}$$

where $n = 2 \sim 3$.

For simplicity, the effective stress acting on the solid phase merely results from *in situ* solidification shrinkage in the solidifying alloy. So-called *in situ* solidification shrinkage means that the deformation of the two-phase zone results from not an external load but the solidification shrinkage itself. Solidification shrinkage β can be evaluated with the liquid and solid densities during solidification:

$$\beta = -\frac{\rho_L - \rho_S}{\rho_S} \tag{10}$$

where ρ_L is liquid density and ρ_S is solid density. Since β is a volume contraction percentage, the linear

strain γ due to solidification shrinkage should approximately be:

$$\gamma \cong \frac{1}{3}\beta \tag{11}$$

The two-phase zone during solidification is generally regarded as a body with visco-elastic-plastic behavior. The incorporation, however, of viscous process into a model of the formation process leads to a great increase in the complexity of the problem. For simplicity, the following discussion concentrates on the simple treatment that considers the two-phase zone as the Kelvin body with visco-elasticity [19, 20], that is:

$$\sigma_S = \eta\dot{\gamma} + E\gamma \tag{12}$$

where η is viscosity, and E is elastic modulus. Substituting Equation 12 into Equation 8, the effective stress acting the solid phase of the matrix is:

$$\sigma' = m(\eta\dot{\gamma} + E\gamma) \tag{13}$$

3. The solidification models

The solidification model here is schematically shown in Fig. 1, where there are insulated walls on the top and the bottom, and a water-cooled chill mold or a sand mold at each side. The different side molds result in two cooling rates during solidification. Table I represents the relation of the cooling rates at the ingot surface and centerline with dimensionless time τ, that is defined as ratio of time t to the final solidification time t_f under the each cooling conditions. For the solidification model of Al-4.5wt%Cu alloy with two-dimension size of 100 mm(height) × 80 mm(width), the final solidification times of the plane castings are 84 sec. for the chill mold and 1245 sec. for the sand mold, respectively. Thermophysical properties of the Al-Cu alloy is listed in Table II. Fig. 2 shows liquid and solid densities of the alloy, which are used to calculate the strain due to *in situ* solidification shrinkage.

TABLE I Cooling rates at different time and positions

dimensionless time	Cooling rate (K/s)			
	sand mold wall		water-cooled chill	
	surface	center	surface	center
0.0	1.1	0.0	6.4	0.0
0.2	0.85	0.45	6.3	0.72
0.4	0.76	0.50	6.16	0.90
0.7	0.63	0.55	5.96	1.10
1.0	0.60	0.58	5.40	2.92

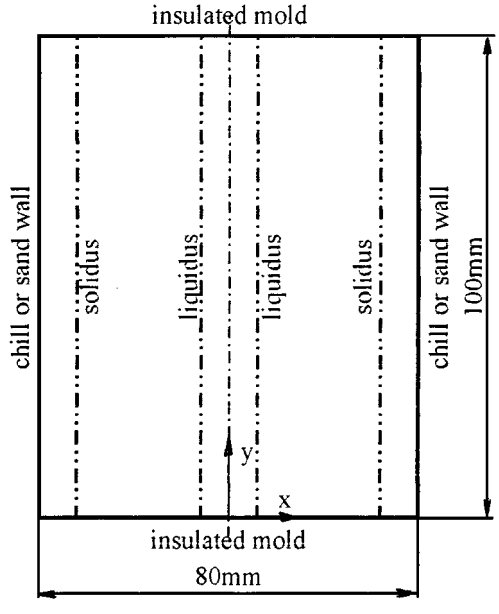

Figure 1 Schematic representation of solidification model of a plane casting.

The temperature field and the positions of the liquidus and the eutectic isotherms for the solidification models are given by [16]:

$$T(|x|, t) = T_E + \frac{(|x| - |x_E|)}{(|x_L| - |x_E|)}(T_L - T_E) \tag{14}$$

$$|x_L(t)| = \frac{L}{2} - b_{Lx}t^q \tag{15a}$$

and

$$|x_E(t)| = \frac{L}{2} - b_{Ex}t^q - a_E \tag{15b}$$

where T is temperature, T_L is liquidus temperature, T_E is eutectic temperature, x_L is position of the liquidus isotherm, x_E is position of the eutectic isotherm, L is length of the ingot, and a_E, b_{Lx}, b_{Ex}, and q are constants in Equation 15, respectively.

The viscosity and the elastic modulus are mainly dependent on temperature. The temperature dependence of the viscosity may be described by [21]:

$$\eta = A\exp\left(\frac{\Delta G_{VIS}}{RT}\right) \tag{16}$$

TABLE II Thermophysical properties of Al-4.5% Cu alloy

compressibility coefficient ($N^{-1}m^2$)	1.45×10^{-9}; [17]
liquidus slope of binary diagram (K/wt %)	−3.4
partition ratio	0.172
liquidus temperature (K)	918.0
melting point of pure solvent (K)	933.0
latent heat (J kg^{-1})	3.89×10^5
specific heat (J $kg^{-1}K^{-1}$)	1.04×10^3

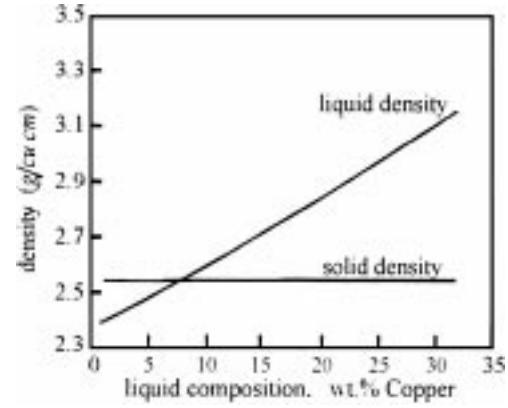

Figure 2 Liquid and solid densities of Al-Cu alloy [15].

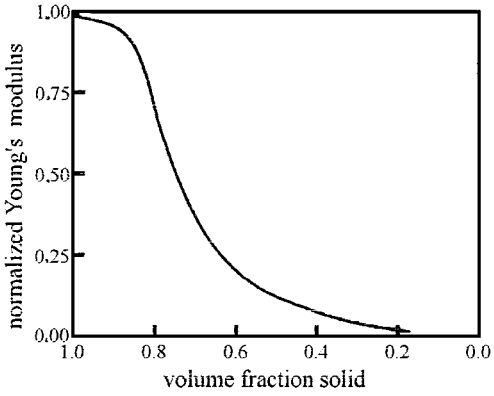

Figure 3 Elastic modulus during solidification of Al-Cu alloy. $E = 17.5$GPa at solidus.

where A is viscosity constant, T is absolute temperature, R is gas constant, and ΔG_{VIS} is activation energy of viscosity. The viscosity increases with decreasing temperature from Equation 16. The elastic modulus also has a similar variation with temperature. The variation of E as a function of volume fraction solid is plotted in Fig. 3.

4. The effective stress distributions at different cooling rates

A viscous element and an elastic element are connected in parallel for the Kelvin model in Equations 12 and 13. The response of this model to an applied stress is that the stress is at first carried entirely by the viscous element. Under the stress, the viscous element then deforms, thus transferring a greater and greater portion of the load to the elastic element [22]. The model approximately represents the deformation behavior of the two-phase zone of a solidifying alloy, that is, the viscous behavior is mostly exhibited in the early stage of solidification, and the elastic behavior gradually rises as solidification proceeds. Thus, Equation 13 can be turned into:

$$\sigma' = \sigma'_V + \sigma'_E \tag{17}$$

where σ'_V is the effective stress due to the viscous behavior, and σ'_E is the effective stress due to the elastic behavior.

Using the chain rule and combining Equations 10 and 11, the strain rate $d\gamma/dt$ in Equation 13 can be written into:

$$\dot{\gamma} = -\frac{m_L}{3\rho_S}\frac{d\rho_L}{dC_L}\varepsilon \tag{18}$$

where m_L is liquidus slope of the alloy binary diagram, and ε is cooling rate during solidification. It is assumed for Equation 18 that ρ_S is regarded as a constant and $d\rho_L/dC_L$ is the slope of the curve in Fig. 2 if the liquidus curve is treated as a straight line. Using the above equation, the viscous element of Equation 13 can be calculated with:

$$\sigma_V{}' = -\frac{mm_L\eta}{3\rho_S}\frac{d\rho_L}{dC_L}\varepsilon \tag{19}$$

The strain rate and the viscous element of the effective stress are related to the cooling rate from Equations 18 and 19.

The relations of the effective stress σ' with the dimensionless time τ at the two cooling rates are shown in Fig. 4. The effective stress at the surface is always larger than that at the centerline. The difference, however, between the stresses at the surface and the centerline changes with cooling rate of the solidification model. For the sand mold, the difference is small in Fig. 4a since the difference of cooling rate throughout the casting is not large. For the water-cooled chill casting, the stress at the surface is obviously larger than that at the centerline since the cooling rates are quite different and solidification at the surface occurs before that at the centerline. Fig. 5 shows the effective stress distributions from the center to the surface at $\tau = 0.6$. the stress gradient along x-direction for the water-cooled chill is greater than the one for the sand mold.

A fluid moving relative to a solid boundary exerts a force on the boundary. This force results from two factors. The first is shear stress due to viscosity and velocity gradient at the boundary surface which gives rise to a force tangential to the surface. The second is a pressure variation along the surface that acts normal to the surface. Moreover, the stress is also resolved into a shear force and a normal force, which exist simultaneously

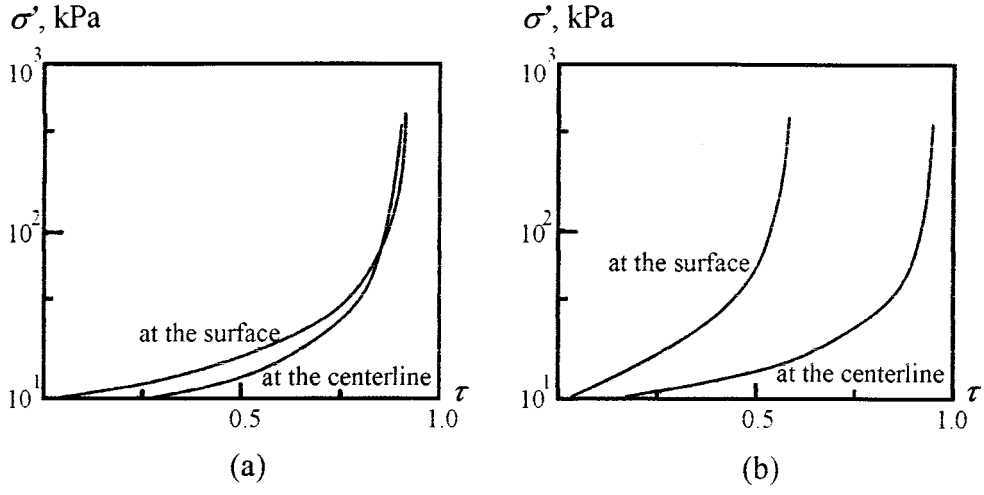

Figure 4 Dependent of the effective stress on dimensionless time at the surface and the centerline of the casting: (a) sand mold wall, (b) chill wall.

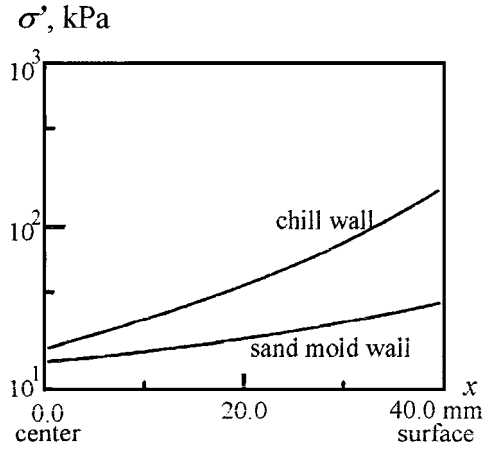

Figure 5 The effective stress distributions of sand mold wall and chill wall castings along *x* direction.

in the solid phase. Shear strain due to the shear stress and normal strain due to the normal stress, which are indicated with not partial derivative but total derivative in Equations 5 and 6, make the solid-phase deformation in the two-phase zone complicated. In order to simplify the problem, the normal strain is merely discussed here. The effective stress acting on the solid phase may also be resolved into shear and normal components relative to isotherms in the two-phase zone, e. g., liquidus and solidus. The normal strain in the two-phase zone results from the normal component of the effective stress. Though this assumption should be considered as an approximation, the main feature of the solid-phase deformation may be emphasized. When the normal strain is merely taken into consideration, Equation 5 becomes:

$$\operatorname{div} \boldsymbol{V}_S' = \frac{1}{U_b}\frac{\partial U_b}{\partial t} \tag{20}$$

For the solidification model as shown in Fig. 1, the isobars of normal stress and contours of constant normal strain are parallel to the chill wall (i. e., *y* direction) since the liquidus and solidus isotherms are, in turn, almost parallel to the chill wall.

5. Discussion

5.1. Interdendritic fluid flow at different cooling conditions

In order to analyze the effect of solid-phase deformation on interdendritic fluid flow, multiplying Equation 3 by $\partial t/\partial T$ gives:

$$\left(\frac{\partial g_S}{\partial t} + \operatorname{div} \boldsymbol{V}_S'\right)\frac{\partial t}{\partial T} = \left(\frac{1-\beta g_L \partial C_L}{1-kC_L\partial T}\right)\left(1+\frac{\boldsymbol{V}_L-\nabla T}{\varepsilon}\right) \tag{21}$$

The quantity inside the first bracket on the right side of the equation is always negative, regardless of the value of $k > 1$ or $k < 1$. According to earlier investigators [15], the different cooling conditions of an ingot can cause three modes of fluid flow in the two-phase zone, i.e., stable flow, intermediate flow, and unstable flow, which are determined by the value of $(\boldsymbol{V}_L - \nabla T)/\varepsilon$: the stable flow at $(\boldsymbol{V}_L - \nabla T)/\varepsilon > 0$ and the unstable flow at $(\boldsymbol{V}_L - \nabla T)/\varepsilon < -1$.

If the normal strain is only taken into account, substituting Equation 20 into the left side of Equation 21:

$$\left(\frac{\partial g_S}{\partial t} + \operatorname{div} \boldsymbol{V}_S'\right)\frac{\partial t}{\partial T} = \frac{\partial g_S}{\partial T} + \frac{1}{U_b}\frac{\partial U_b}{\partial T} \tag{22}$$

With decreasing temperature, the volume of the two-phase zone U_b decreases for the most metals and, so the term $\partial U_b/\partial T$ is, as a rule, larger than zero.

When $(\boldsymbol{V}_L - \nabla T)/\varepsilon > 0$, the right side of Equation 21 is less than zero, and there is:

$$\frac{\partial g_S}{\partial T} < -\frac{1}{U_b}\frac{\partial U_b}{\partial T} \tag{23}$$

or

$$\frac{\partial g_S}{\partial T} < 0, \quad \text{and,} \quad \left|\frac{\partial g_S}{\partial T}\right| > \frac{1}{U_b}\frac{\partial U_b}{\partial T} \tag{24}$$

Equation 24 shows that the volume fraction solid increases with decreasing temperature and the variation of the volume fraction solid due to the solid-phase deformation cannot play an effective role, that is, the term, $1/U_b(\partial U_b/\partial T)$ can not make the left side of Equation 21 less than zero. So, the flow remains stable.

When $(\boldsymbol{V}_L - \nabla T)/\varepsilon < -1$, the right side of Equation 21 is greater than zero, and there is:

$$\frac{\partial g_S}{\partial T} + \frac{1}{U_b}\frac{\partial U_b}{\partial T} > 0 \tag{25}$$

Equation 25 indicates that the unstable flow may result from two terms: $\partial g_S/\partial T$ and $1/U_b(\partial U_b/\partial T)$. Since the term $1/U_b(\partial U_b/\partial T)$ is always positive during solidification, there are two cases for the value of $\partial g_S/\partial T$:

(1) $-1/U_b(\partial U_b/\partial T) < \partial g_S/\partial T \leq 0$, that is, it is still $\partial g_S/\partial T \leq 0$, and this means that the unstable flow in the two-phase zone results from the solid-phase deformation, that is, only the term $1/U_b(\partial U_b/\partial T)$ makes the left side of Equation 20 greater than zero;

(2) $\partial g_S/\partial T > 0$, and the unstable flow can result jointly from the effective stress and the gravity force acting on a fluid with various density.

When the cooling rate is large and the solidifying isotherm moves fast, there is not enough time to produce the strain if the effective stress is less than the strength of the solidifying alloy itself. This is the case as shown with Equation 24. It should be noted that a residual stress may be left in the solidified ingot though no strain occurs. With decreasing the cooling rate and slowing the movement of the isotherm, the effective stress may be relaxed by the deformation of the two-phase zone, and plays a role in forming the "channel space" filled with the unstable flow [14, 15]. The velocity distributions of interdendritic fluid flow can be calculated on the basis of the local solute redistribution equation, velocity equation, and pressure equation [14]. Fig. 6 shows the calculated velocity profiles in the two-phase

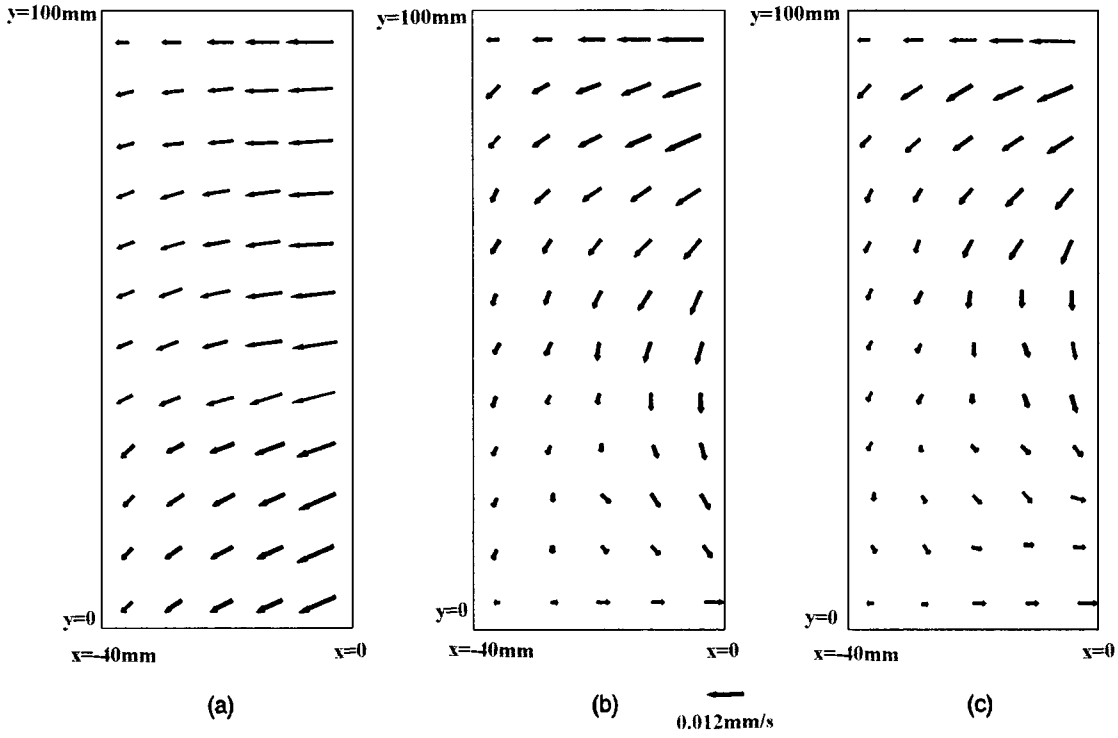

Figure 6 Calculated velocity profiles in the two-phase zone with: (a) chill wall, (b) sand wall without action of the stress, and (c) sand wall with action of the stress.

zone of the alloy under the two different cooling conditions, i.e., the chill wall and the sand mold wall. For the chill wall, the fluid flows counter to the movement of the isotherm, Fig. 6a. For the sand mold wall, it can be seen by compared Fig. 6b and c that the effective stress may strengthen the back-flow towards the ingot centerline.

5.2. Deformation mismatch

In order to interpret the season why inhomogeneous distributions of cooling rate in a solidifying alloy result in thermal residual stress, we turn Equations 5 and 6 into:

$$\operatorname{div} \boldsymbol{V}_S' = \frac{1}{U_b}\frac{dU_b}{dt} = -\alpha\frac{d\sigma'}{dT}\varepsilon \qquad (26)$$

Fig. 7 shows the distributions of $\operatorname{div} \boldsymbol{V}_S'$ along x direction at two different time. As mentioned above, the term

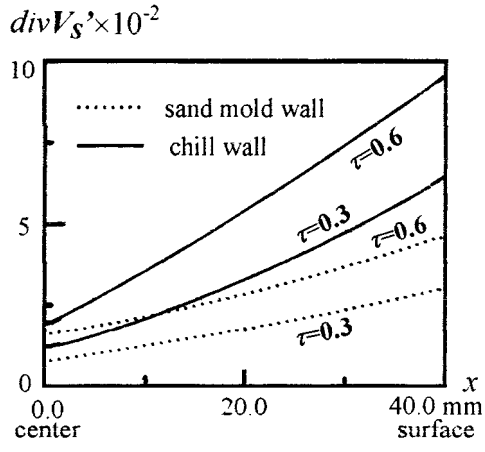

Figure 7 The distributions of relative volume rate at two different dimensionless time.

$\operatorname{div} \boldsymbol{V}_S'$ means the relative volume rate at a local volume element. Two neighboring local volume elements of the solidifying alloy are shown in Fig. 8a. So-called deformation mismatch means the difference of the relative volume rate between the two neighboring local volume elements due to the different cooling conditions. No deformation mismatch, on the other hand, occurs between the two neighboring local volume elements if their relative volume rates are equal. So, the deformation mismatch is a parameter similar to not strain but strain rate. It can be seen from Equation 26 and Fig. 7 that the different relative volume rates due to the different cooling rates result in the deformation mismatch among the various volume elements. The greater the difference between the cooling rate distributions, the greater is the deformation mismatch is. The mismatch for the model with the water-cooled chill is larger than that with the sand mold wall. It is suggested that the deformation mismatch give rise to thermal residual stress in a solidifying alloy when the mismatch is not relaxed.

In Fig. 8a, the deformation mismatch of the two elements results from their different cooling rates. The relative volume rate is related not to the value of the effective stress itself but to the variation of the effective stress with time according to Equation 6. The deformation mismatch produced by the cooling conditions at every time interval is small, and a part of it may be relaxed at the early stage of solidification. The formation, however, of thermal residual stress is an accumulation of the mismatch with time. The accumulation starts from the solidification stage. So, the deformation mismatch both during and after solidification should be considered in analysis of the thermal residual stresses of a material in the solidification processing. If the material of the two volume elements in Fig. 8b is different,

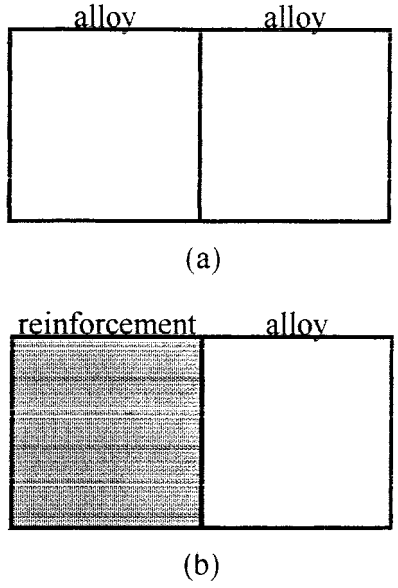

Figure 8 Comparison of unreinforced alloy and reinforced alloy: (a) the mismatch is from cooling conditions of neighboring elements with the same alloy, and (b) the mismatch is from both different property and cooling conditions of the neighboring elements with the different materials.

e.g., at reinforcement/matrix interface of a composite, the mismatch may result from the different thermal properties of the two elements as well as the cooling rates.

6. Conclusions

1. The term div $\boldsymbol{V}_S'$, defined as the relative volume rate at a local volume element, is used to evaluate the deformation in the two-phase zone of a solidifying alloy. The term is dependent on history of the effective stress acting on the solid phase. On the basis of Equation 26 in which the term is related to cooling rate during solidification, it is easy to discuss the effect of the cooling rate on the deformation in the two-phase zone.

2. The difference between the stresses at the surface and the centerline changes with the cooling rate of the solidification model. For the sand mold, the difference between the stresses at the surface and the centerline is small since the difference of cooling rate everywhere is not large. For the water-cooled chill, the stress at the surface is larger than that at the centerline since the cooling rates are very different and solidification at the surface is prior to that at the centerline.

3. When the cooling rate is large and the solidifying isotherm moves fast, there is not enough time to produce the strain if the effective stress is less than the strength of the solidifying alloy itself. It should be noted that a residual stress may be left in the solidified ingot though no strain occurs. With decreasing the cooling rate and slowing the movement of the isotherm, the effective stress may be relaxed by the deformation of the two-phase zone and play a role in forming the "channel space" filled with the unstable flow. For the chill wall, the fluid flow is contrary to the movement of the isotherm in the direction, and for the sand mold wall, the effective stress may strengthen the back-flow towards the ingot centerline (Fig. 6).

4. So-called deformation mismatch means the difference of the relative volume rate between the two neighboring local volume elements due to the different cooling conditions and is a parameter similar to not strain but strain rate. It can be seen from Equation 26 and Fig. 7 that the different relative volume rate due to the different cooling rates result in the deformation mismatch among the various volume elements. The greater the difference between the cooling rate distributions is, the greater the deformation mismatch is. The mismatch for the model with the water-cooled chill is larger than that with the sand mold wall. Formation of thermal residual stress is an accumulation of the mismatch with time. It is suggested that the deformation mismatch give rise to thermal residual stress in a solidifying alloy when the mismatch is not relaxed.

References

1. M. C. FLEMINGS, *Metall Trans.* **22A** (1991) 957.
2. D. J. LLOYD, *Int. Mater. Rev.* **39** (1994) 1.
3. J . CAMPBELL, *Trans. AIME* **242** (1968) 264.
4. *Idem., ibid.* **242** (1968) 268.
5. R. A. ROSENBERG, M. C. FLEMINGS and H. F. TAYLOR, *Trans. AFS* **28** (1960) 518.
6. D. B. SPENCER, R. MEHRABIAN and M. C. FLEMINGS, *Metall. Trans.* **3** (1972) 1925.
7. M. C. FLEMINGS, "Solidification Processing" (McGraw-Hill, New York, NY, 1974) p. 252.
8. W. KURZ and D. J. FISHER, "Fundamentals of Solidification" (Trans. Tech. Publications, Switzerland, 1989).
9. A. MUNITZ, S. P. ELDER-RANDALL and R. ABBASCHIAN, *Metall. Trans.* **23A** (1992) 1817.
10. Q. YU and Y. ZHOU, *Int. J. Heat Mass Transfer* **34** (1991) 843.
11. N. B. BRYSON, *Light Metal* (1972) 429.
12. H. D. BRODY and P. WISNIEWSKI, in "Modeling of Casting and Welding Processes IV," edited by A. F. Giamei and G. J. Abbaschian (TMS, 1988) p. 351.
13. K. Y. KIM, H. SAKUTA, T. SUZUKI, T. UMEDA, T. KOBAYASHI and M. TATEISHI, in "Modeling of Casting, Welding and Advanced Solidification Processes V," edited by M. Rappaz, M. R. Ozgu and K. W. Mahin (TMS, 1991) p. 259.
14. Q. YU, M. MAKHLOUF and D. APELIAN, *Int. J. Heat Mass Transfer* **38** (1995) 31.
15. R. MEHRABIAN, M. KEANE and M. C. FLEMINGS, *Metall. Trans.* **1** (1970) 1209.
16. L. MAPLES and D. R. POIRIER, *ibid.* **15B** (1984) 163.
17. J. BEAR, "Dynamics of Fluid in Porous Media" (American Elsevier, New York, 1972) p. 52.
18. K. TERZAGHI, "From Theory to Practice in Soil Mechanics" (Wiley, New York, 1960).
19. F. S. SHERMAN, "Viscous Flow" (McGraw-Hill, New York, 1990).
20. A. J. FLETCHER, "Thermal Stress and Strain in Heat Treatment" (Elsevier, London, 1989).
21. G. H. GEIGER and D. R. POIRIER, "Transport Phenomena in Metallurgy" (Addison-Wesley Publ. Co., New York, 1981).
22. W. N. FINDLEY, J. S. LAI and K. ONARAN, "Creep and Relaxation of Nonlinear Viscoealstic Materials" (North-Holland Publ. Co., New York, 1976).

Received 30 March 1998
and accepted 11 April 2000